© 2014. Published by The Company of Biologists Ltd | The Journal of Experimental Biology (2014) 217, 1946-1954 doi:10.1242/jeb.098228

RESEARCH ARTICLE

Biomechanics of substrate boring by fig wasps

Lakshminath Kundanati and Namrata Gundiah*

ABSTRACT

Female insects of diverse orders bore into substrates to deposit their eggs. Such insects must overcome several biomechanical challenges to successfully oviposit, which include the selection of suitable substrates through which the ovipositor can penetrate without itself fracturing. In many cases, the insect may also need to steer and manipulate the ovipositor within the substrate to deliver eggs at desired locations before rapidly retracting her ovipositor to avoid predation. In the case of female parasitoid ichneumonid wasps, this process is repeated multiple times during her lifetime, thus testing the ability of the ovipositioning apparatus to endure fracture and fatigue. What specific adaptations does the ovipositioning apparatus of a female ichneumonoid wasp possess to withstand these challenges? We addressed this question using a model system composed of parasitoid and pollinator fig wasps. First, we show that parasitoid ovipositor tips have teeth-like structures, preferentially enriched with zinc, unlike the smooth morphology of pollinator ovipositors. We describe sensillae present on the parasitoid ovipositor tip that are likely to aid in the detection of chemical species and mechanical deformations and sample microenvironments within the substrate. Second, using atomic force microscopy, we show that parasitoid tip regions have a higher modulus compared with regions proximal to the abdomen in parasitoid and pollinator ovipositors. Finally, we use videography to film wasps during substrate boring and analyse buckling of the ovipositor to estimate the forces required for substrate boring. Together, these results allow us to describe the biomechanical principles underlying substrate boring in parasitoid ichneumonid wasps. Such studies may be useful for the biomimetic design of surgical tools and in the use of novel mechanisms to bore through hard substrates.

KEY WORDS: Ovipositor, Zinc, Hardness, Hertz contact theory, SEM, Sensillae, Buckling

INTRODUCTION

The ability of female insects to find and access suitable oviposition sites is a key challenge for the successful growth and propagation of new hatchlings. Female insects of many diverse orders, such as locusts (Order: Orthoptera), damsel flies (Order: Odonata), wasps (Order: Hymenoptera) and others deposit their eggs in a substratum that either provides them with protection (Kalogianni, 1995; Vincent, 1976; Matushkina and Gorb, 2007; Vincent and King, 1995; Quicke et al., 2004) or serves as a nursery for maturing eggs while also providing nourishment to the developing larvae. For such insects, substrate boring is an essential feature of the ovipositioning behaviour, requiring them to overcome several biomechanical constraints. Substrate-boring insects typically possess externally occurring valve-like structures in their ovipositor, which penetrate and cut the host substrate to enable deposition of their eggs. The ovipositor itself consists of three parts including two ventral valves and one dorsal valve interlocked to allow sliding between the valves, which permits boring and egg deposition (Quicke et al., 1998). In contrast, internal structures of the insect body pierce, and steer the ovipositor to deliver eggs to the substrate (Vincent and King, 1995; Quicke et al., 1999). In members of Hymenoptera, such as wasps, the ovipositor may also act as a sting to inject venom into other live hosts (Rahman et al., 1998; Gal and Libersat, 2010) using a cocktail of neuromodulators to ensure that the host behaviour is altered to benefit the parasitic brood. Multiple ovipositions within substrates using the same bored hole may require the insect to steer and manipulate eggs through the ovipositor guided by mechanosensory and chemosensory feedback. Specialized mechanosensory campaniform sensillae, distributed at various locations on the surface of the insect cuticle (Sivinski and Aluja, 2003), are capable of detecting nanometre displacements. Rhythmic mechanosensory feedback from campaniform sensillae may be essential for initiating the ovipositor motor patterns through the differential response of ovipositor hair sensillae to tactile stimulation (Zill and Moran, 1981). In addition to mechanical signals, chemotactic stimuli are also known to aid parasitoid wasps in locating areas containing host larvae.

From a materials perspective, the insect ovipositor is a fascinating system whose properties are not fully understood. The ovipositors of wood-boring wasps show little evidence of wear and tear of their cutting parts (Quicke et al., 1998). It is hypothesized that the presence of zinc and manganese hardens the insect cuticle and permits it to cut through hard substrates such as wood (Quicke et al., 1998; Hillerton and Vincent, 1982; Fawke et al., 1997). However, the distribution of metals in insect ovipositors and their direct correlation with local material properties has not been explored to date. Here, using the fig wasp system, we employed a scanning electron microscope (SEM) with an energy dispersive X-ray analysis detector to characterize the composition and morphology of the fig wasp pollinator and parasitoid ovipositor system and coupled these measurements with atomic force microscope (AFM) indentation experiments to quantify their local material properties. To assess deformations of parasitoid ovipositors during egg laying, we filmed the wasps while they were boring through fig substrates. These films were then quantified to measure the buckling properties of the ovipositor. Together, our studies identify key morphological adaptations in both pollinator and parasitoid fig wasp species that help overcome the challenges faced by these insects during oviposition. Such studies may have wide-ranging applications for the development of tissue probes during robotic assisted surgeries, needle biopsies using functionally graded tools, the design of biomimetic structures through the use of embedded holes as strain sensors (Skordos et al., 2002), and increasing the toughness of tools with large aspect ratios.

Department of Mechanical Engineering, Indian Institute of Science, Bangalore 560012, India.

*Author for correspondence (namrata@mecheng.iisc.ernet.in)

Received 10 October 2013; Accepted 17 February 2014

The Journal of Experimental Biology

The Journal of Experimental Biology (2014) doi:10.1242/jeb.098228

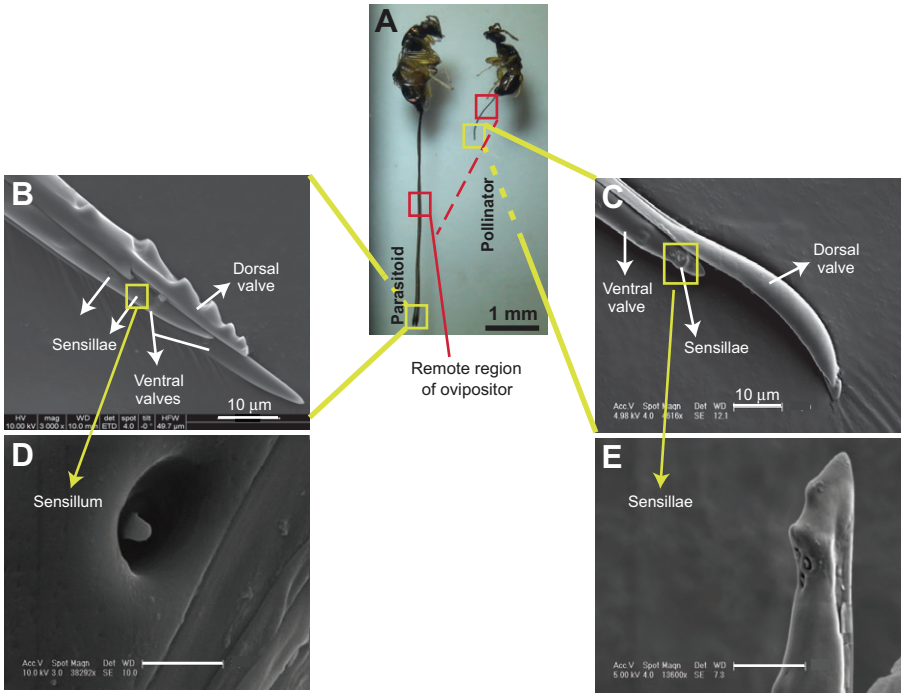

Fig. 1. Parasitoid and pollinator fig wasp ovipositors. (A) Images showing a clear difference in the body size and length of ovipositors in the parasitoid (*Apocrypta* spp.) and pollinator (*Ceratosolen fusciceps*) fig wasp species used in the study. (B,C) Scanning electron micrographs showing morphological differences in the tip regions of the dorsal valves from representative parasitoid (B) and pollinator (C) wasp ovipositors. Remote regions of the ovipositor refer to regions far from the tip. (D) Uniformly distributed coeloconic sensillae are present on the ventral valves of parasitoid ovipositors. (E) In contrast, a high density of campaniform sensillae is observed to be clustered in the ventral valves of pollinator ovipositors.

RESULTS

Differences in the morphology and composition of fig wasp pollinator and parasitoid ovipositors

Scanning electron micrographs showed striking differences in the morphologies of pollinator and parasitoid ovipositors, which may be adaptations to the different requirements during oviposition (Fig. 1). Pollinators oviposit in flowers present in the fig syconium (Ghara et al., 2011) whereas parasitoids bore through the relatively hard fig syconia to oviposit. Both dorsal and ventral valves of pollinator ovipositors are relatively smooth with a spoon-like morphology in contrast to the sharp and long parasitoid ovipositors with teeth-like projections at the tip, which increase in size towards the proximal end. In addition, campaniform sensillae appear concentrated at tips of pollinator ovipositor ventral valves (Fig. 1C,E), whereas coeloconic and campaniform sensillae are more uniformly distributed along the length of the ventral valves of parasitoids (Fig. 1B,C) as compared with the tip regions alone. The diameter of pollinator ovipositors, measured using five different SEM micrographs, at regions far from the tip and proximal to the abdomen, referred to as ‘remote’ for brevity, was 9.43±0.42 µm (N=5) and that near the tip regions was 9.54±0.60 µm. In contrast, the diameters of the parasitoid ovipositors increased to 14.32±0.63 µm (N=5) at the tips compared with 9.73±1.40 µm in the remote regions.

Both pollinator and parasitoid species have three valves interlinked by rail guide-like structures using dovetail joints (Fig. 2) that aid in the inter-sliding of the individual valves through an olistheter mechanism (Quicke and Fitton, 1995). Thus, the substrates for oviposition are clearly different in the two species although the mechanisms used by them may be similar. Micrographs also showed the presence of one set of sensillae on the pollinator ovipositor whereas the parasitoid ovipositor had more than one type of sensilla. In an earlier study, sensillae on the parasitoid ovipositor were identified to be basiconic, coeloconic and campaniform (Ghara et al., 2011).

Pollinator and parasitoid species were assayed for the possible presence of transition metals at the ovipositor tip and remote regions using an energy dispersive X-ray analysis (EDS) detector in the SEM. We did not find calcium or other metals in pollinator ovipositors but there was an increased presence of zinc in parasitoid tips alone. Representative curves corresponding to pure zinc control, pollinator and parasitoid materials are shown in Fig. 3. X-ray spectra from the pure zinc pellet and the parasitoid tip regions show a perfect overlap in peaks corresponding to the K and L lines of zinc compared with other samples. Using X-ray counts obtained in the different regions, our data show that parasitoid ovipositor specimens had a weight percentage of zinc of 7.19±3.8% (N=42) in the tip regions, which was significantly higher (P<0.05) than that in pollinator and parasitoid remote regions (<1%; N=10). Because weight percentages of zinc in remote regions are within errors obtained using EDS detectors, we do not give exact numbers for

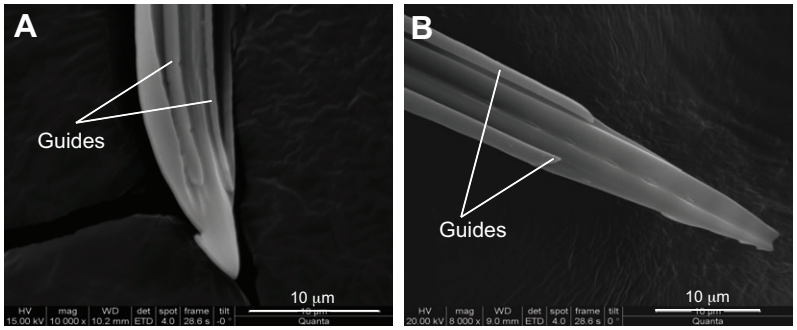

Fig. 2. Scanning electron microscope (SEM) images showing the presence of rail guides on the dorsal valves of the pollinator and parasitoid ovipositors. (A) Pollinator ovipositor; (B) parasitoid ovipositor. The rail guides aid in the sliding of the valves during oviposition.

The Journal of Experimental Biology (2014) doi:10.1242/jeb.098228

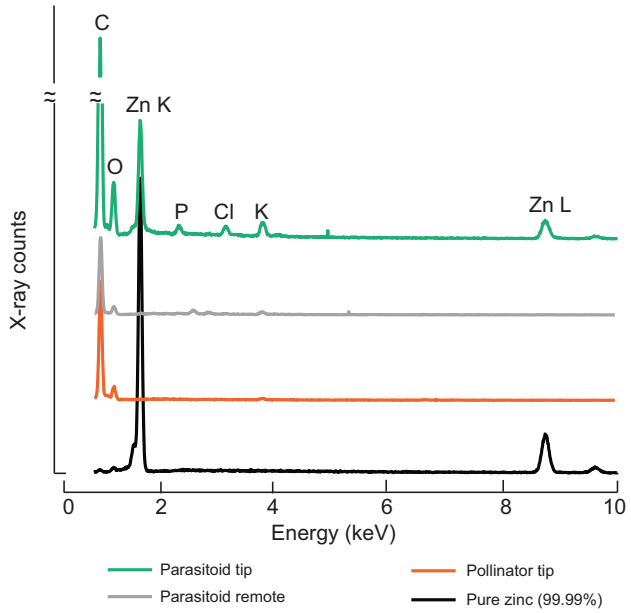

Fig. 3. Representative energy dispersive X-ray analysis (EDS) spectra. The spectra show overlapping peaks of zinc lines (K and L) from parasitoid ovipositor tip and remote regions, pollinator remote regions, and a pure zinc pellet (99.99%) used as a control.

values <1%. Based on these results, we hypothesize that the presence of zinc exclusively in the cutting regions of the parasitoid tips results in an increased hardness to aid boring through substrates.

Mechanical properties of pollinator and parasitoid ovipositors

Images of pollinator and parasitoid ovipositor specimens, obtained using the tapping mode in AFM, show clear differences in the surface topography of parasitoid ovipositors in the tip and remote regions proximal to the abdomen, which correlate with corresponding SEM images (Fig. 4). Pit-like areas are abundant in remote regions of parasitoid ovipositors, which are clearly absent in the tip regions of parasitoid and pollinator wasps. The pit diameter in remote regions of the parasitoid ovipositors was 275.3±57.6 nm (N=9) at four locations for each AFM image used in this study. We do not, however, see any substructure to the pit-like regions in these images. To quantify the material properties of the ovipositor samples, we used the indentation mode in the AFM. Because of possible errors associated with the measurements due to high surface roughness (R_a), we used the automated software in the AFM prior to the measurement of material properties to quantify R_a for the ovipositor surfaces. Surface roughness of pollinator and parasitoid ovipositors in the remote regions was 2.34±1.37 nm (N=9) and 2.43±0.79 nm (N=9), respectively. In contrast, roughness of the tip parasitoid region was significantly higher (9.67±4.92 nm; N=9) than the corresponding remote region of parasitoid ovipositors (P<0.05). Typical force–depth curves from experiments performed on a single pollinator and parasitoid ovipositor specimen are shown in Fig. 5Bi and 5Bii, respectively. We obtained a highly reproducible mechanical response for the pollinator cuticle samples. In contrast, data from the tip regions of parasitoid ovipositors show a larger variance between individual indents, which may be related to higher roughness values in these regions. Further, tip regions of parasitoid specimens have a clearly stiffer material response, seen by the reduced penetration depth, compared with remote regions.

To quantify these responses, we fitted the experimentally obtained force–depth relationships to theoretically calculated values using a Hertzian contact mechanics model and a non-linear least squares fit method as described in Materials and methods. There were no significant differences (P<0.05) in elastic moduli (E), calculated using Poisson's ratio ν=0.37, from the remote region of pollinator ovipositors (0.92±0.16 GPa) compared with corresponding remote regions from parasitoid ovipositors (0.73±0.19 GPa) (Table 1). However, we found significantly higher values for moduli (1.42±0.29 GPa) for the tip regions of parasitoid ovipositors in comparison with data from remote regions of parasitoid and pollinator ovipositor materials (P<0.05). Finally, we used these measured properties to calculate the material hardness for the different regions in parasitoid and pollinator ovipositors. Although we did not see any differences in moduli corresponding to the remote regions of parasitoid and pollinator ovipositors, we note

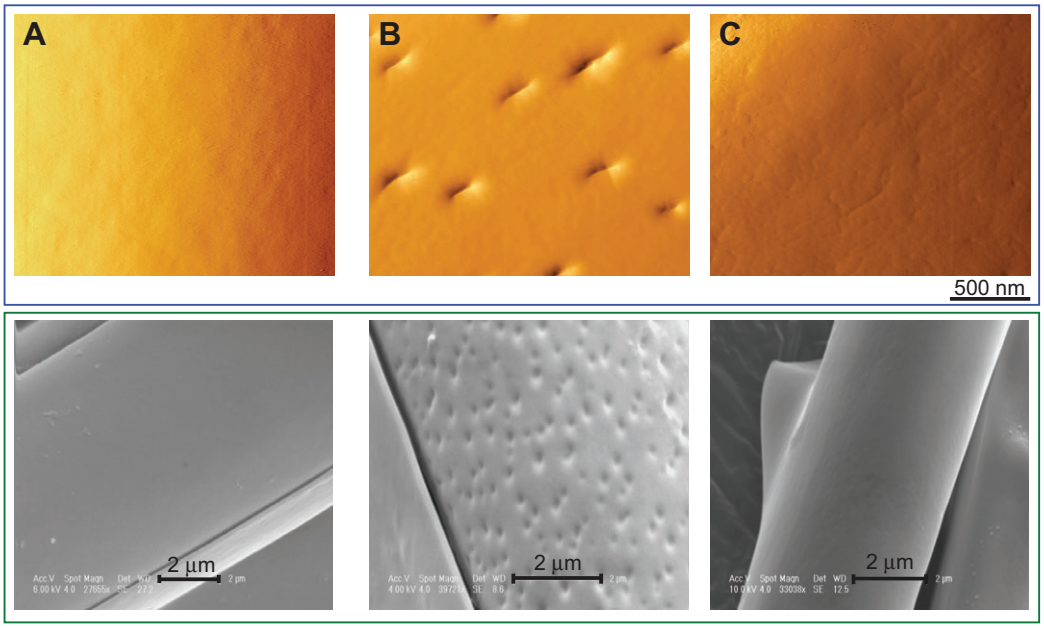

Fig. 4. Surface topography of pollinator and parasitoid ovipositors. Images were obtained using the tapping force mode in an atomic force microscope (AFM; upper panels). (A) Remote regions in a pollinator ovipositor show a relatively smooth surface. (B) In contrast, the corresponding region of a parasitoid ovipositor shows the presence of uniform pits. (C) The tip region of a parasitoid ovipositor. SEM images (lower panels) are also included to show the corresponding surface topographies, obtained at lower magnification, which agree with the results from AFM.

The Journal of Experimental Biology (2014) doi:10.1242/jeb.098228

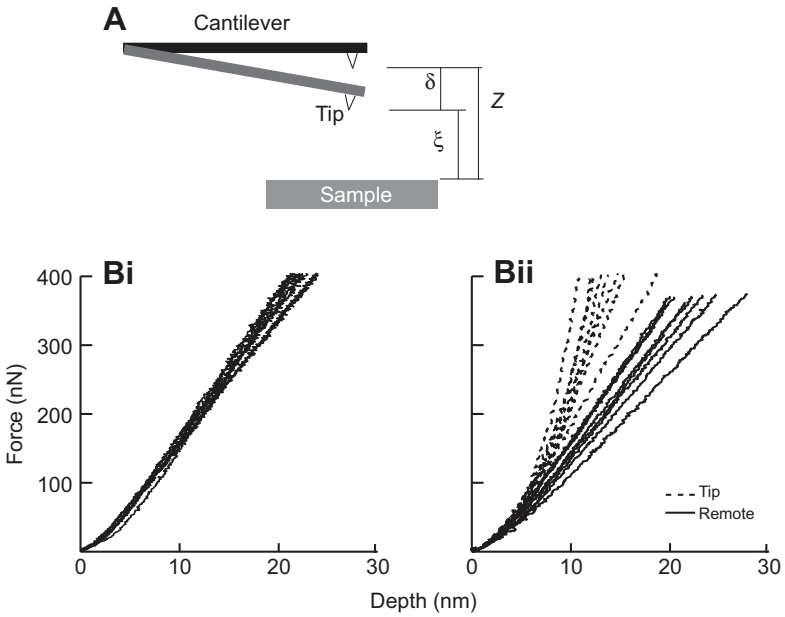

Fig. 5. Atomic force microscopy system showing the cantilever tip that was used to estimate properties of the cuticle substrate. (A) Schematic diagram showing the indentation mode in AFM used to quantify the material properties of the substrate. Indentation depth: δ=*Z*–ξ; measured force: *F*=*k*ξ, where ξ is cantilever deflection, *Z* is Piezo displacement and *k* is cantilever stiffness. (B) Force–depth relationships for a sample in a remote region of pollinator ovipositors (i, *N*=7) and those corresponding to the tip and remote regions of parasitoid ovipositors (ii, *N*=8). These data show higher material stiffness for parasitoid tips compared with remote regions.

significant differences in their calculated hardness. Hardness values (0.50±0.11) for the parasitoid tip were higher (P<0.05) than those for the corresponding remote region (0.32±0.06). We also found significant differences in the hardness of the pollinator ovipositor (0.18±0.02) compared with the hardness of parasitoid material (P<0.05).

Parasitoid wasp oviposition on fig substrates

Parasitoids patrol the fig syconia and tap the surface periodically with their antennae to locate embedded hosts within the substrate (Broad and Quicke, 2000). Through such a vibrational sounding behaviour the insect may use a combination of chemical and mechanical cues to identify a suitable substrate for oviposition. Upon selection of the site for oviposition, the insect raises her abdomen and anchors her ovipositor to the substrate using her hindlegs (supplementary material Movie 1). Finally, she uses a vibratory mechanism to drill through the syconium. We found that the total time taken for each oviposition varied between 109 and 744 s (N=29; mean 297±156 s), which may depend on substrate stiffness, the number of eggs deposited during a single penetration and the location of the pollinator larvae. Abdominal displacements occur in the plane perpendicular to the axis of drilling. Following sheath removal and initial anchoring, we observed periodic buckling of the insect ovipositor at several time points during a single penetration event into the substrate for oviposition. This causes the insect to partially retract the ovipositor about 2–7 times whilst using the same bored hole for oviposition. Oviposition videos were digitized and the buckling length of the ovipositor was determined to be 0.48±0.09 mm (N=12) using ImageJ software (Fig. 6). Micrographs from five other animals were used to obtain ovipositor diameters from which the critical buckling force was estimated (Eqn 9 in Materials and methods). Using the average values for the modulus, buckling length and diameter of ovipositors, we calculated that 6.9 μN of force was required to cause ovipositor buckling.

DISCUSSION

The ovipositor design facilitates egg laying by attenuating penetration forces to cut through the substrate, while allowing for its manipulation within the substrate, and minimizing structural damage to the ovipositor. The primary aim of our study was to quantify the structure–function relationship in insect ovipositors to understand how it enables insects to bore through substrates of different stiffness. There are four main implications of this work. First, we

Table 1. Elastic moduli of the pollinator and parasitoid ovipositors

	Pollinator – remote		Parasitoid – remote		Parasitoid – tip	
Sample	No. of indents	*E* (GPa)	No. indents	*E* (GPa)	No. indents	*E* (GPa)
1	7	0.71±0.03	7	1.13±0.25	7	1.73±0.37
2	9	1.11±0.13	8	0.62±0.14	8	1.39±0.23
3	10	0.77±0.13	8	0.79±0.12	6	1.66±0.38
4	8	0.87±0.1	8	0.59±0.1	6	1.16±0.19
5	9	0.80±0.1	10	0.57±0.16	8	1.80±0.51
6	7	0.89±0.05	8	0.77±0.21	6	1.48±0.47
7	10	0.88±0.06	8	0.84±0.21	8	1.29±0.49
8	9	1.13±0.2	8	0.76±0.19	9	1.40±0.41
9	9	1.08±0.17	8	0.51±0.08	6	0.87±0.12
Mean		0.92±0.16		0.73±0.19		1.42±0.29

Elastic moduli (*E*) were calculated using the force–depth curves performed at a number of different locations on each specimen, denoted as 'indents', using the AFM (see Materials and methods). Data are reported as means ± s.d.

The Journal of Experimental Biology (2014) doi:10.1242/jeb.098228

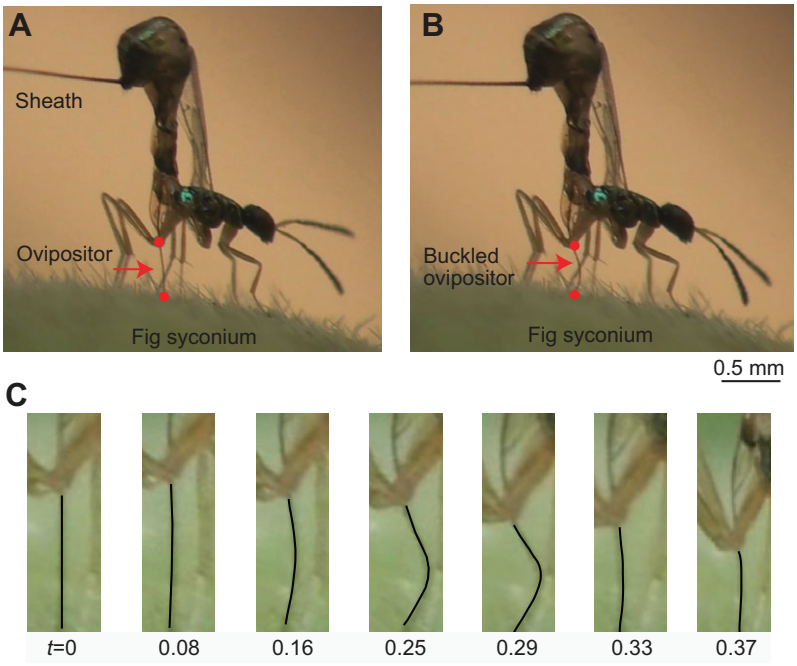

Fig. 6. Snapshots showing the parasitoid wasp ovipositing on a fig substrate. Lengths of the ovipositors are shown (A) just before buckling and (B) during buckling. (C) The time-lapse sequence of images is shown for a single recording to illustrate ovipositor buckling. *t* is time (s).

identified how the morphology of the pollinator and parasitoid ovipositors has adapted to the challenges faced by insects during ovipositioning in substrates of varied stiffness. Parasitoid ovipositor tips have a higher content of the transition metal zinc compared with the cuticle elsewhere on the ovipositor. In addition, various chemosensory and mechanosensory sensillae are present to help in the detection of chemicals and in strain sensing. Second, zinc-containing regions in the parasitoid ovipositor tips have higher moduli compared with remote regions proximal to the abdomen. Third, the ovipositor contains a region that allows buckling, thus preventing it from breaking on a hard surface during the drilling process. Calculation of the buckling forces, through a Euler buckling analysis of the videography data, were used to estimate the penetration forces generated by the insect during oviposition. Fourth, our studies suggest that insects use an oscillatory mechanism to cut through the substrate. Rail guides present between the dorsal and ventral valves of the ovipositors aid in the sliding of the valves during motion.

Comparison of the structure and composition of parasitoid and pollinator ovipositors

The morphology of fig wasp pollinator and parasitoid ovipositors shows clear differences in the ovipositor structure (Fig. 1). Pollinator fig wasps have a spoon-like structure in contrast to the sharp and long ovipositors with teeth-like projections at the parasitoid ovipositor tip that are probably adapted for oviposition. Earlier studies examined the ovipositor morphology in various parasitic Hymenoptera and suggested that many morphological features in ovipositor structures are matched to specific host types (Quicke et al., 1999; Rahman et al., 1998; Fawke et al., 1997; Broad and Quicke, 2000; LeRalec et al., 1996). These studies also showed the presence of transition metals, such as zinc, manganese and calcium, in the tips of the ovipositors using X-ray microanalysis. For instance, the ovipositors of the wood-boring wasps *Megalyra fasciipennis* and *Diasthaphenus* sp. contain zinc levels greater than 5% weight on serrations at the apex of the ovipositor tip (Vincent and King, 1995; Quicke et al., 1998). In other parasitic wasps like *Gabunia* sp. and *Heterospilus prosopidi*, the presence of calcium in the ovipositor tips enables high wear resistance through biomineralization (Quicke et al., 2004). Most other reported wasp species have higher amounts of zinc and/or manganese in their ovipositors (Quicke et al., 1998; Vincent and King, 1995; Polidori et al., 2013; Quicke et al., 2004). Similarly, the presence of transition metals in larvae mandibles of *Stegobium paniceum* and *Gibbium aequinoctiale* species of beetles aids in boring into hard seeds as oppposed to others without metals, which are incapable of seed boring (Morgan et al., 2003). The presence of transition metals in insect cuticle and mandible is hypothesized to increase material hardness to permit cutting through hard substrates with minimal wear (Schofield et al., 2002; Schofield et al., 2003; Lichtenegger, 2003; Quicke et al., 1998; Hillerton and Vincent, 1982; Fawke et al., 1997). Although repeated use of the ovipositor when boring through stiff substrates is expected to cause increased wear in the interacting surfaces, the ovipositors of wood-boring wasps show little evidence of wear and tear of their cutting parts (Quicke et al., 1998).

We used an AFM to image the ovipositor surface and also characterize the material properties using an indentation mode. The topology of the insect cuticle is significantly different in tip and remote regions of parasitoid ovipositors (Fig. 4) compared with the smooth regions of the pollinator cuticle. The ovipositor surface has a smoother region with roughness of only a few nanometres in the remote regions of parasitoid and pollinator ovipositors. However, pit-like indents present in the remote regions of parasitoid ovipositors are clearly absent in pollinator ovipositors. The pit dimensions, measured using SEM images at over 20 locations each, were about 251.07±21.59 nm (N=3) in length and appear in remote regions of the parasitoid ovipositor alone. The presence of rough pit-like regions, called pore canals, has been reported in the cuticle of beetles; they extend through the thickness of the cuticle and are hypothesized to aid in the transfer of wax for waterproofing (Gunderson and Schiavone, 1989). Chitin nanofibres form the bulk of the cuticle material and are moulded around hole-like structures during development. Hierarchical structures, composed of essentially brittle materials combine to produce exceptionally tough and fracture-resistant hybrid materials like bone and tooth dentin. Microvoids in these materials act as local crack arrestors, thereby

The Journal of Experimental Biology (2014) doi:10.1242/jeb.098228

generating higher toughness (Imbeni et al., 2005). Because parasitoid ovipositors generate large forces, compared with those of pollinators, to pierce relatively hard substrates, the presence of pit-like regions in the proximal ovipositor regions may enhance their toughness to withstand forces during boring.

Material properties of pollinator and parasitoid ovipositors

Indentation measurements performed using AFM show clear differences in force–displacement data from the tip and remote regions of parasitoid ovipositors (Fig. 5). However, we did not see any significant differences in measurements from remote regions of parasitoid and pollinator ovipositors located proximal to the insect abdomen. Experimental force–displacement results were fitted to a Hertzian contact mechanics model to quantify differences in material hardness as described earlier (Table 1). Our results show that tip regions of parasitoid ovipositors have a significantly higher modulus and a correspondingly higher hardness than the remote regions of parasitoid and pollinator ovipositors, respectively. The higher moduli for parasitoid tips compared with remote regions correlates with the presence of zinc in tip regions of the ovipositors. The parasitoid ovipositor tips are also sclerotized as observed by the darkened cuticle at the tips compared with the remote regions (Ghara et al., 2011). During sclerotization, epidermal cells of the cuticle secrete phenolic compounds that lead to crosslinking of proteins and removal of water from the cuticle matrix (Vincent and Wegst, 2004). Andersen showed that secondary reactions caused by removal of water from the insect cuticle play a dominant role in contributing to the stiffness of the material as compared with processes that remove phenols through chemical treatment (Andersen, 2010). In this study, we prepared ovipositors for mechanical experiments using an ethanol dehydration procedure that leads to a stiffer material response compared with native fresh insect cuticle (Müller et al., 2008; Barbakadze et al., 2006; Schofield et al., 2002; Klocke and Schmitz, 2011). Ethanol storage of insect specimens was, however, unavoidable because of limitations with acquiring insects and in sample preparation for measurement of mechanical properties using AFM. Because ethanol treatment may not affect the bound zinc from cuticle material, our results showing the increased hardness of parasitoid ovipositor tips compared with their remote regions are nevertheless important to demonstrate the role of zinc and sclerotization in cuticular hardness.

Broomell and co-workers probed the relationship between the presence of various transition metals, such as zinc, copper and manganese, and the hardness and stiffness of biological materials through differential zinc chelation and its replacement with different metals in a model marine polychaete annelid jaw, *Nereis virens* (Broomell et al., 2006; Broomell et al., 2008). Using nanoindentation of treated jaw material, they showed an increased hardness in materials that had about 8% weight of zinc. The increase in hardness of insect cuticle was also hypothesized to be related to the crosslinking of histidine-rich protein fibre bundles in the biomaterial mediated through zinc. Higher material hardness of ant mandibles also correlates with the presence of metal in articulating surfaces (Schofield et al., 2002). EDS used in our study is a semi-quantitative method for estimation of zinc, but revealed clear differences in the composition of parasitoid ovipositor tips compared with other non-cutting regions of the ovipositor. However, there is little direct evidence of increased material hardness due to the presence of transition metals, such as zinc, reported in any insect ovipositor specimens, especially ones with dimensions of about 10 µm such as that reported in our study. These are the only structure–property correlations reported in Hymenoptera that provide direct confirmation for the increased elastic modulus of zinc-containing regions compared with remote regions devoid of zinc.

Biomechanical considerations in substrate boring

The parasitoid ovipositor buckles frequently during oviposition (Fig. 6) without fracture, demonstrating the flexibility of its structure. We estimated critical buckling load generated by the parasitoid during oviposition to be about 6.9 µN, calculated using a length of 0.48 mm, a radius of the ovipositor at the remote regions of 9.73 µm and an elastic modulus of 0.73 GPa, which is the maximum force generated by insects during oviposition. To facilitate multiple ovipositions using the same bored hole and to select the path of least resistance when confronted with different substrate densities, it may be necessary to steer the ovipositor inside the syconium. Thus, a combination of tip hardening to reduce wear and increased ovipositor flexibility are two of the strategies employed in the design of the ovipositor to achieve successful boring through substrates. We observed the presence of three valves composed of two ventral valves interlocking with a single dorsal valve for the pollinator and parasitoid fig wasp species, similar to other ovipositors reported for Hymenoptera. Rail guide structures (Fig. 2) on the dorsal and ventral valves allow for translation of the ovipositor structures through an olistheter mechanism, which has been described in other Hymenoptera (Quicke and Fitton, 1995). Fig. 7 shows the curved trajectory taken by the ovipositor inside the plant syconium, which traverses a differential stiffness on its path inside the substrate. This was obtained by decapitating the insect at

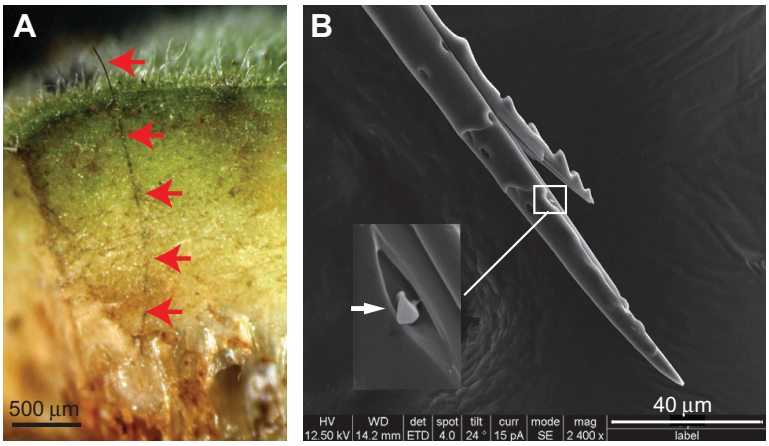

Fig. 7. Steerability of parasitoid ovipositor in the fig substrate. (A) Tracings showing the curved path taken by the ovipositor in the fig substrate that illustrate manoeuvring of the ovipositor inside the substrate. (B) SEM images of the parasitoid ovipositor showing the dorsal and ventral valves that comprise the ovipositor. The inset shows a possible mechanical stopper sensillum, indicated by the white arrow, which may be useful in limiting displacement between the two ovipositor parts.

the end of oviposition. The curvature of the length of the dorsal valve compared with that of the ventral valve during sliding may aid in changing the direction of the ovipositor tip inside the substrate. In earlier studies, projections close to the apex on the ventral valves were hypothesized to act as stoppers to avoid the two ventral valves extending beyond the dorsal valve (Quicke and Fitton, 1995). To limit maximum sliding movement between the dorsal and ventral ovipositor structures in the olistheter mechanism, while aiding movement inside the syconium, we explored the possible role of a currently unidentified sensilla, located about 40–55 µm from the ovipositor tip on the ventral valve, inside a groove in the ventral side along the length of the parasitoid ovipositor (Fig. 7). We did not see such a sensilla at any other location along the groove of the two parasitoid valves or in the pollinator ovipositor (Ghara et al., 2011). Recent investigations have used the deployment of steerable flexible tools in surgery through an insect-inspired drilling process (Frasson et al., 2010; Ko et al., 2011). Hence, the presence of sensillae may aid in maintaining a steering offset to help manoeuvre the tool inside the substrate. Although such a process seems plausible, additional experiments are required to establish the role of this sensillum as a mechanical stopper.

In conclusion, we used a combination of scanning electron microscopy with indentation experiments from AFM to characterize the structure–function relationships in insect ovipositor materials. Through such methods, we show unique morphological adaptations in the ovipositors of parasitoid fig wasps to aid boring through hard substrates. Together, our findings reveal novel mechanisms used by insects in boring and also suggest the placement of multiple chemical and mechanical sensors that facilitate such processes.

MATERIALS AND METHODS

Model insect systems

Fig wasps were selected as a model in this study because interactions between various wasp species and the host plant (*Ficus racemosa*) present a well-characterized system for substrate boring (Ghara et al., 2011). Fig trees on the Indian Institute of Science campus provided ready access to wasps. The community of wasp species co-existing with *F. racemosa* consists of one pollinating species, *Ceratosolen fusciceps* (Mayr), which uses fig syconium to deposit eggs in addition to six non-pollinating species. Of the non-pollinating wasps, parasitoids (*Apocrypta* sp.2, *Apocrypta westwoodi* Grandi) identify viable fig substrates housing developing pollinator larvae and oviposit their eggs, which mature into adult parasitoid wasps that leave the syconium (Fig. 1).

Fig syconia present in the wasp emerging D-phase were placed in a container to allow the natural emergence of all wasp species. Insects were collected and stored in 70% ethanol until use. The ovipositors along with their protective covering sheaths were dissected from the abdomen and carefully separated. Individual ovipositor samples were dried in an oven at 60°C for 20 min and prepared for microscopy.

Scanning electron microscopy with EDS detector to quantify ovipositor morphology and composition

Because of the relatively small dimensions of insect ovipositors, dehydration or freeze drying was not necessary for SEM imaging studies. Prepared ovipositors were carefully mounted on double-sided carbon tape (Electron Microscopy Sciences, USA), stuck on an aluminium stub, and placed in a desiccator to avoid contamination. Specimens were transferred to a sputter coater (Bal-Tec SCD 500, Liechtenstein), the chamber was purged thrice with argon and the samples were coated with gold. A SEM (Quanta 200 ESEM, FEI, The Netherlands) was used with accelerating voltages between 5 and 20 kV. Ovipositors were imaged and their surface features were characterized at different scales. ImageJ software was used for all dimensional quantification reported in this study (Abràmoff and Magalhães, 2004).

To quantify the elemental composition of ovipositors, specimens were mounted on carbon tape without any gold coating and imaged in the SEM using an EDS detector. Spectra were collected using an accelerating voltage of 20 kV and at a working distance of 10 mm. Identification of individual peaks in a given spectrum was performed using custom-written software (Genesis, FEI) and a pure zinc sample was used as calibration material in this technique. The weight percentage of zinc quoted in the study is reported using a standardless method inbuilt in the software.

AFM for characterization of surface morphology and quantification of material properties

AFM is widely used to image specimens, when used in tapping mode, and also to evaluate local nanoscale mechanical properties, using indentation mode, for a variety of materials including metals and polymers (Capella and Dietler, 1999). In this method, a microfabricated cantilever is brought towards the specimen using a piezoelectric translation stage and the deflection of the cantilever tip (ξ) into the substrate is obtained. The force on the sample is measured using cantilever tip stiffness (k). Vertical translation of the sample towards the cantilever tip provides the approach curve used to obtain indentation of the tip with the sample (Fig. 5A). Data from force–displacement curves were used to characterize the material behaviour using a Hertzian contact mechanics model. In this, the force (F) due to interactions between two spherical linear elastic bodies, representing the cantilever tip and the substrate with which it is in contact, is given by:

$$F = A\delta^{\frac{3}{2}}, \quad (1)$$

where δ is the indentation depth, and A is a constant for a given tip geometry with spherical radius R:

$$A = \frac{4E\sqrt{R}}{3(1-\nu^2)}. \quad (2)$$

Here, ν is Poisson's ratio for the sample and E is the elastic modulus of the material.

Material hardness (H) is given as ratio of the maximum load (P_{max}) in the force–depth curve to the projected area $A_c=2\pi Rh_c$ (where h_c is the contact depth) as:

$$H = \frac{P_{max}}{A_c}. \quad (3)$$

The final depth of indentation (δ_{max}) is used to calculate A_c (Oliver and Pharr, 1992).

Experimental investigation of ovipositor specimens using the AFM

To determine the material properties and surface morphologies of ovipositor specimens, we used the AFM (Veeco dI Innova, USA) in both indentation and tapping modes. To permit easy visualization of the ovipositor specimens in the AFM without affecting mechanical measurements, ovipositor samples were mounted on a thin layer of Erase-X correction fluid applied to the AFM puck (Bhushan and Chen, 2006). All experiments were performed using a diamond-like carbon (DLC)-coated silicon tip (stiffness 5 N m^{-1}, Veeco, USA) with a set voltage of 3.65 V and scanning frequency of 0.5 Hz to image about 4 µm^2 area with resolution of 256×256 pixels in a controlled environment (22–24°C). Roughness of the ovipositor surface was measured using height images following a first order level-set method using SPM software along three lines.

To quantify the elastic modulus of the ovipositor, we used AFM in the indentation mode (Fig. 5). Locations for indentation were selected based on surface topography images. Rates of approach and retraction of the cantilever tip were maintained at 0.1 µm s^{-1} and the cantilevers were calibrated after every set of experiments to determine the spring constant (k), using the Sader thermal tuning method, for quantification of forces using voltage measurements. Sensitivity of the AFM cantilever, defined as the rate of piezoelectric movement per unit cantilever deflection (nm V^{-1}), was calculated as the inverse slope of the approach curve on a standard silicon sample. Raw data from the approach curve were converted to force–depth relationships using MATLAB (v 7.8.0.347 R2009a). The minimum force

was identified as the contact point of the tip with the surface in this study. Data obtained prior to this value were removed as there are no interactions between the tip and sample in this region. Voltage (V) corresponding to cantilever movement was converted to cantilever deflection (ξ) using sensitivity measurements (m) and is given by:

$$\xi = mV, \quad (4)$$

where m is the cantilever sensitivity. The depth of penetration (δ) is calculated using piezo position (Z) and cantilever deflection (ξ) as:

$$\delta = Z - \xi. \quad (5)$$

The applied force on the sample is hence calculated using a Hookean elastic response as:

$$F = k\xi. \quad (6)$$

Experimental force–depth data from AFM experiments were fitted to a Hertzian contact mechanics model (Eqns 1–3) using a non-linear least squares optimization method employing a Levenberg–Marquardt algorithm using the function *lsqnonlin* in MATLAB. In this method, at least five different initial guesses were used to arrive at converged solutions and the optimizations were terminated when either the tolerance placed on the objective function was less than 1E–10 or the tolerance placed on the estimated parameter values was less than 1E–8. Values corresponding to the maximum value of r^2 from various optimizations are reported as the global converged values in this study. To calculate the elastic moduli from the converged values of A (Eqn 2), we used the average tip radius of the cantilevers from a data sheet and assumed a Poisson's ratio of ν=0.37. Statistical analyses to test for differences in the different groups were performed using ANOVA with Bonferroni comparison using the multcompare function in MATLAB. P<0.05 is considered significant.

Videography of parasitoid wasp oviposition

Parasitoid oviposition was recorded on fig substrates in the field using a video camera (Sony HDR XR500) with an objective lens (Olympus 1XPF) kept at a distance of ~28 cm for suitable magnification. A thin wire of known diameter (0.83 mm), placed in the field of view following successful oviposition, was used for calibration. Images taken prior to buckling were used to measure the ovipositor length present between the hinge and the distal end of the ovipositor in the syconium surface. Buckling length (L) was estimated from the images using ImageJ and the critical load (P_{cr}) for buckling was calculated using the Euler buckling equation. In this method, we model the ovipositor as a cylindrical column and use the measured modulus (E), buckling length (L) and radius of the ovipositor (R) to obtain P_{cr} as:

$$P_{cr} = \frac{\beta\pi^2 EI}{L^2}. \quad (7)$$

Here, I is the area moment of inertia [where I=(πR^4)/16] and β=2 for a free end loading of the column.

Acknowledgements

We are grateful to (the late) Prof. Sanjay Kumar Biswas for use of the AFM and to Ms Savitha and Ms Haritha for help with experiments. We also thank Mr Vaibhav Agrawal for assistance with analysing AFM data and to Dr Renee Borges for preliminary discussions during early stages of this work.

Competing interests

The authors declare no competing financial interests.

Author contributions

N.G. conceived and designed the study, supervised experiments and data analysis, interpreted results and wrote the manuscript. L.K. carried out experiments and analysed the data. Contributions from other researchers for instrument use, technical discussions, and help with programming are individually acknowledged. Both authors agree and approve of the contents in this manuscript.

Funding

N.G. acknowledges the Department of Science and Technology for the Ramanujan fellowship and research grant [RJN-42] that supported part of this work.

Supplementary material

Supplementary material available online at
http://jeb.biologists.org/lookup/suppl/doi:10.1242/jeb.098228/-/DC1

References

Abràmoff, M. D. and Magalhães, P. J. (2004). Image processing with ImageJ. *Biophotonics Intl.* **11**, 36-42.
Andersen, S. O. (2010). Insect cuticular sclerotization: a review. *Insect Biochem. Mol. Biol.* **40**, 166-178.
Barbakadze, N., Enders, S., Gorb, S. and Arzt, E. (2006). Local mechanical properties of the head articulation cuticle in the beetle *Pachnoda marginata* (Coleoptera, Scarabaeidae). *J. Exp. Biol.* **209**, 722-730.
Bhushan, B. and Chen, N. (2006). AFM studies of environmental effects on nanomechanical properties and cellular structure of human hair. *Ultramicroscopy* **106**, 755-764.
Broad, G. R. and Quicke, D. L. J. (2000). The adaptive significance of host location by vibrational sounding in parasitoid wasps. *Proc. R. Soc. Lon. B* **267**, 2403-2409.
Broomell, C. C., Mattoni, M. A., Zok, F. W. and Waite, J. H. (2006). Critical role of zinc in hardening of *Nereis* jaws. *J. Exp. Biol.* **209**, 3219-3225.
Broomell, C. C., Zok, F. W. and Waite, J. H. (2008). Role of transition metals in sclerotization of biological tissue. *Acta Biomater.* **4**, 2045-2051.
Cappella, B. and Dietler, G. (1999). Force-distance curves by atomic force microscopy. *Surf. Sci. Rep.* **34**, 5-104.
Fawke, J. D., McClements, J. G. and Wyeth, P. (1997). Cuticular metals: quantification and mapping by complementary techniques. *Cell Biol. Int.* **21**, 675-678.
Frasson, L., Ko, S. Y., Turner, A., Parittotokkaporn, T., Vincent, J. F. V. and Rodriguez y Baena, F. (2010). STING: a soft-tissue intervention and neurosurgical guide to access deep brain lesions through curved trajectories. *Proc. Inst. Mech. Eng. H* **224**, 775-788.
Gal, R. and Libersat, F. (2010). A wasp manipulates neuronal activity in the sub-esophageal ganglion to decrease the drive for walking in its cockroach prey. *PLoS ONE* **5**, e10019.
Ghara, M., Kundanati, L. and Borges, R. M. (2011). Nature's Swiss Army knives: ovipositor structure mirrors ecology in a multitrophic fig wasp community. *PLoS ONE* **6**, e23642.
Gunderson, S. and Schiavone, R. (1989). The insect exoskeleton: a natural structural composite. *JOM* **41**, 60-62.
Hillerton, J. E. and Vincent, J. F. V. (1982). The specific location of zinc in insect mandibles. *J. Exp. Biol.* **101**, 333-336.
Imbeni, V., Kruzic, J. J., Marshall, G. W., Marshall, S. J. and Ritchie, R. O. (2005). The dentin-enamel junction and the fracture of human teeth. *Nat. Mater.* **4**, 229-232.
Kalogianni, E. (1995). Physiological properties of wind-sensitive and tactile trichoid sensilla on the ovipositor and their role during oviposition in the locust. *J. Exp. Biol.* **198**, 1359-1369.
Klocke, D. and Schmitz, H. (2011). Water as a major modulator of the mechanical properties of insect cuticle. *Acta Biomater.* **7**, 2935-2942.
Ko, S. Y., Frasson, L. and Rodriguez, F. (2011). Closed-loop planar motion control of a steerable probe with a 'Programmable Bevel' inspired by Nature. *IEEE Trans. Robot.* **27**, 970-983.
LeRalec, A., Rabasse, J. M. and Wajnberg, E. (1996). Comparitive morphology of the ovipositor of some parasitic Hymenoptera in relation to characteristics of their hosts. *Can. Entomol.* **128**, 413-433.
Lichtenegger, H. C. (2003). Response to comment on 'high abrasion resistance with sparse mineralization: copper biomineral in worm jaws'. *Science* **301**, 1049.
Matushkina, N. and Gorb, S. (2007). Mechanical properties of the endophytic ovipositor in damselflies (Zygoptera, Odonata) and their oviposition substrates. *Zoology (Jena)* **110**, 167-175.
Morgan, T. D., Baker, P. and Kramer, K. J. (2003). Metals in mandibles of stored product insects : do zinc and manganese enhance the ability of larvae to infest seeds? *J. Stored Prod. Res.* **39**, 65-75.
Müller, M., Olek, M., Giersig, M. and Schmitz, H. (2008). Micromechanical properties of consecutive layers in specialized insect cuticle: the gula of *Pachnoda marginata* (Coleoptera, Scarabaeidae) and the infrared sensilla of Melanophila acuminata (Coleoptera, Buprestidae). *J. Exp. Biol.* **211**, 2576-2583.
Oliver, W.C., Pharr, G.M. (1992). An improved technique for determining hardness and elastic modulus using load and displacement sensing indentation experiments. *J. Mater. Res.* **7**, 1564-1583.
Oliver, W. C. and Pharr, G. M. (2004). Measurement of hardness and elastic modulus by instrumented indentation: advances in understanding and refinements to methodology. *J. Mater. Res.* **19**, 3-20.
Polidori, C., García, A. J. and Nieves-Aldrey, J. L. (2013). Breaking up the wall: metal-enrichment in ovipositors, but not in mandibles, co-varies with substrate hardness in gall-wasps and their associates. *PLoS ONE* **8**, e70529.
Quicke, D. L. J. and Fitton, M. G. (1995). Ovipositor steering mechanisms in parasitic wasps of the families Gasteruptiidae and Aulacidae (Hymenoptera). *Proc. R. Soc. B* **261,** 99-103.
Quicke, D. L. J., Wyeth, P., Fawke, J. D., Basibuyuk, H. H. and Vincent, J. F. V. (1998). Manganese and zinc in the ovipositors and mandibles of hymenopterous insects. *Zool. J. Linn. Soc.* **124**, 387-396.

Quicke, D. L. J., Leralec, A. and Vilhelmsen, L. (1999). Ovipositor structure and function in the parasitic Hymenoptera with an exploration of new hypotheses. *Atti dell'Accademia Nazionale Italiana di Entomologia, Rendiconti* **47**, 197-239.
Quicke, D. L. J., Palmer-Wilson, J., Burrough, A. and Broad, G. R. (2004). Discovery of calcium enrichment in cutting teeth of parasitic wasp ovipositors (Hymenoptera: Ichneumonoidea). *Afr. Entomol.* **12**, 259-264.
Rahman, M. H., Fitton, M. G. and Quicke, D. L. J. (1998). Ovipositor internal microsculpture in the Braconidae (Insecta, Hymenoptera). *Zool. Scr.* **27**, 319-332.
Schofield, R. M., Nesson, M. H. and Richardson, K. A. (2002). Tooth hardness increases with zinc-content in mandibles of young adult leaf-cutter ants. *Naturwissenschaften* **89**, 579-583.
Schofield, R. M., Nesson, M. H., Richardson, K. A. and Wyeth, P. (2003). Zinc is incorporated into cuticular 'tools' after ecdysis: the time course of the zinc distribution in 'tools' and whole bodies of an ant and a scorpion. *J. Insect Physiol.* **49**, 31-44.
Sivinski, J. and Aluja, M. (2003). The evolution of ovipositor length in the parasitic Hymenoptera and the search for predictability in biological control. *Fla Entomol.* **86**, 143-150.
Skordos, A., Chan, P. H., Vincent, J. F. V. and Jeronimidis, G. (2002). A novel strain sensor based on the campaniform sensillum of insects. *Philos. Trans. R. Soc. A* **360**, 239-253.
Vincent, J. F. V. (1976). How does the female locust dig her oviposition hole? *J. Ent. A* **50**, 175-181.
Vincent, J. F. V. and King, M. J. (1995). The mechanism of drilling by wood wasp ovipositors. *Biomimetics* **3**, 187-201.
Vincent, J. F. V. and Wegst, U. G. K. (2004). Design and mechanical properties of insect cuticle. *Arthropod Struct. Dev.* **33**, 187-199.
Zill, S. N. and Moran, D. T. (1981). The exoskeleton and insect proprioception. *J. Exp. Biol.* **94**, 57-75.